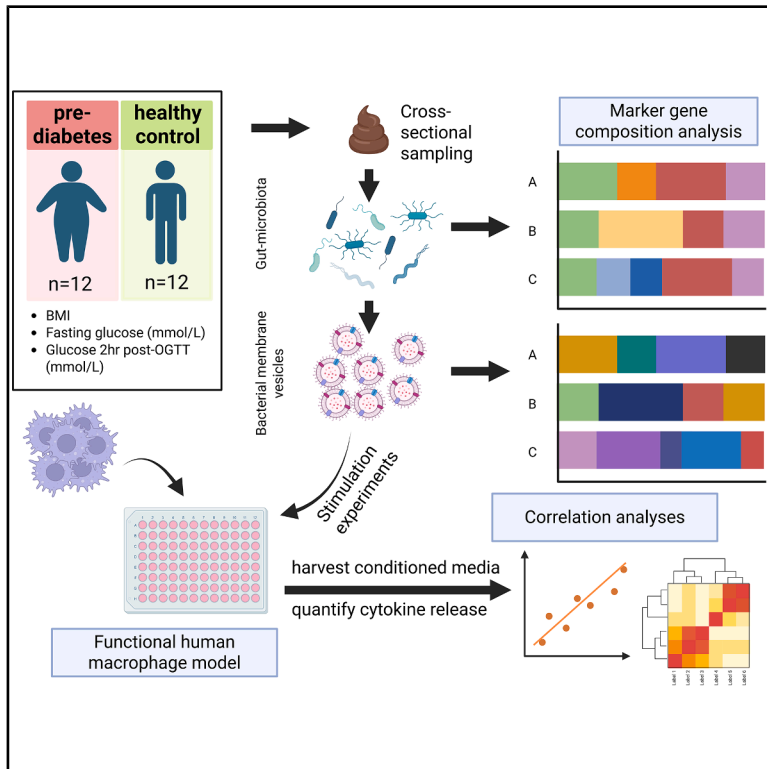


# Gut-derived bacterial membrane vesicles in prediabetes: Vesicle composition dictates inflammatory properties

## Graphical abstract



## Authors

Jari Verbunt, Lisa Mennens, Johan Jocken, Emanuel E. Canfora, Ellen E. Blaak, Paul Savelkoul, Frank Stassen

## Correspondence

f.stassen@maastrichtuniversity.nl

## In brief

Medicine; Bacteriology; Diabetology

## Highlights

- 16S rRNA-based bacterial compositions differ from those of vesicles within a fecal sample
- Prediabetes does not associate with compositional differences in bacteria or vesicles
- Vesicles enriched in Verrucomicrobiae signatures are less inflammatory
- Vesicles enriched in Oscillospiraceae and Lachnospiraceae are more inflammatory



## Article

# Gut-derived bacterial membrane vesicles in prediabetes: Vesicle composition dictates inflammatory properties

Jari Verbunt,<sup>1,2</sup> Lisa Mennens,<sup>2,3</sup> Johan Jocken,<sup>2</sup> Emanuel E. Canfora,<sup>2</sup> Ellen E. Blaak,<sup>2</sup> Paul Savelkoul,<sup>1</sup> and Frank Stassen<sup>1,4,\*</sup>

<sup>1</sup>Department of Medical Microbiology, Infectious Diseases & Infection Prevention, School of Nutrition and Translational Research in Metabolism (NUTRIM), Maastricht University Medical Center+, Maastricht 6229 HX, the Netherlands

<sup>2</sup>Department of Human Biology, School of Nutrition and Translational Research in Metabolism (NUTRIM), Maastricht University Medical Center+, Maastricht 6229 ER, the Netherlands

<sup>3</sup>Rehabilitation Research Center (REVAL), Faculty of Rehabilitation Sciences, Hasselt University, Hasselt 3590, Belgium

<sup>4</sup>Lead contact

\*Correspondence: [f.stassen@maastrichtuniversity.nl](mailto:f.stassen@maastrichtuniversity.nl)

<https://doi.org/10.1016/j.isci.2026.115088>

## SUMMARY

Systemic inflammation relates to the pathophysiology of metabolic diseases such as obesity or type 2 diabetes. Understanding aberrant microbiota-host interactions is essential for comprehending their pathogenesis. Gut bacteria produce bacterial membrane vesicles (bMVs) reflecting bacterial metabolism and activity. Importantly, in animal models, these vesicles can reach organs and affect metabolism by inducing inflammation. We investigated feces-derived gut bacteria and bMVs in participants diagnosed with prediabetes and in healthy controls. Vesicle and bacterial DNA repertoires were found to be vastly different, with Gram-negative bacterial taxa dominating at the vesicle level (*Alistipes*, *Barnesiella*) and Gram-positive taxa (*Anaerostipes*, *Collinsella*) dominating at the bacterial level. We observed no compositional differences between participant-phenotype groups. Strikingly, vesicle repertoires characterized by elevated proportional abundance of Lachnospiraceae and Oscillospiraceae DNA were more proinflammatory, whereas the opposite was observed for vesicles rich in Akkermansiaceae DNA. These results may improve our understanding of microbe-host interactions relevant to metabolic and inflammatory diseases.

## INTRODUCTION

The intestinal microbiome, a diverse community consisting of trillions of microorganisms, plays a crucial role in maintaining host health.<sup>1</sup> This microbial ecosystem regulates numerous physiological processes, including digestion, modulation of the immune system, pathogen defense and the regulation of satiety and mood.<sup>1–4</sup> A disturbance in the composition or function of the microbes inhabiting the lower intestinal tract has been implicated in diseases such as inflammatory bowel disease (IBD),<sup>5</sup> dementia,<sup>6</sup> obesity,<sup>2,7</sup> and type 2 diabetes (T2D).<sup>2,8</sup> In recent years, the influence of the microbiota on metabolic health has been extensively studied to help develop procedures for microbiota modulation toward an increased cardiometabolic health.

Interkingdom communication between gut microbes and their human host occurs via numerous pathways. With regard to metabolic health, the microbiota facilitate energy acquisition from otherwise indigestible fibers, thereby producing short-chain fatty acids (SCFAs) such as acetate, propionate, and butyrate.<sup>9</sup> These SCFAs can exit the intestinal lumen to

reach metabolic organs such as the liver, adipose tissue, and skeletal muscle, where they help modulate energy homeostasis.<sup>2,9</sup> They possess anti-inflammatory properties and constitute the main source of energy for the colonocytes that form the epithelial lining of the colon, thereby supporting gut barrier function.<sup>2</sup>

In addition to gut-derived bacterial metabolites, the gut microbiota also produce bacterial membrane vesicles (bMVs) that can mediate interkingdom communication.<sup>10,11</sup> These membrane-delimited nanoparticles are produced by nearly all bacteria throughout their life cycle, as part of their natural biology as well as in response to stress and external cues.<sup>12,13</sup> They confer bacterial properties by encompassing various bioactive molecules, such as bacterial toxins, metabolites, nucleic acids, lipids, and proteins.<sup>10,14</sup> Their carriage of bacterial DNA allows the characterization of these vesicles by means of the identification of bacterial producer strains.<sup>15,16</sup> Importantly, bacterial membrane vesicles have been found to be able to disseminate functional DNA, such as antibiotic resistance genes.<sup>17,18</sup> The membrane bilayer herein shields the vesicle's cargo from nuclease activity,<sup>19</sup> and, upon contact with



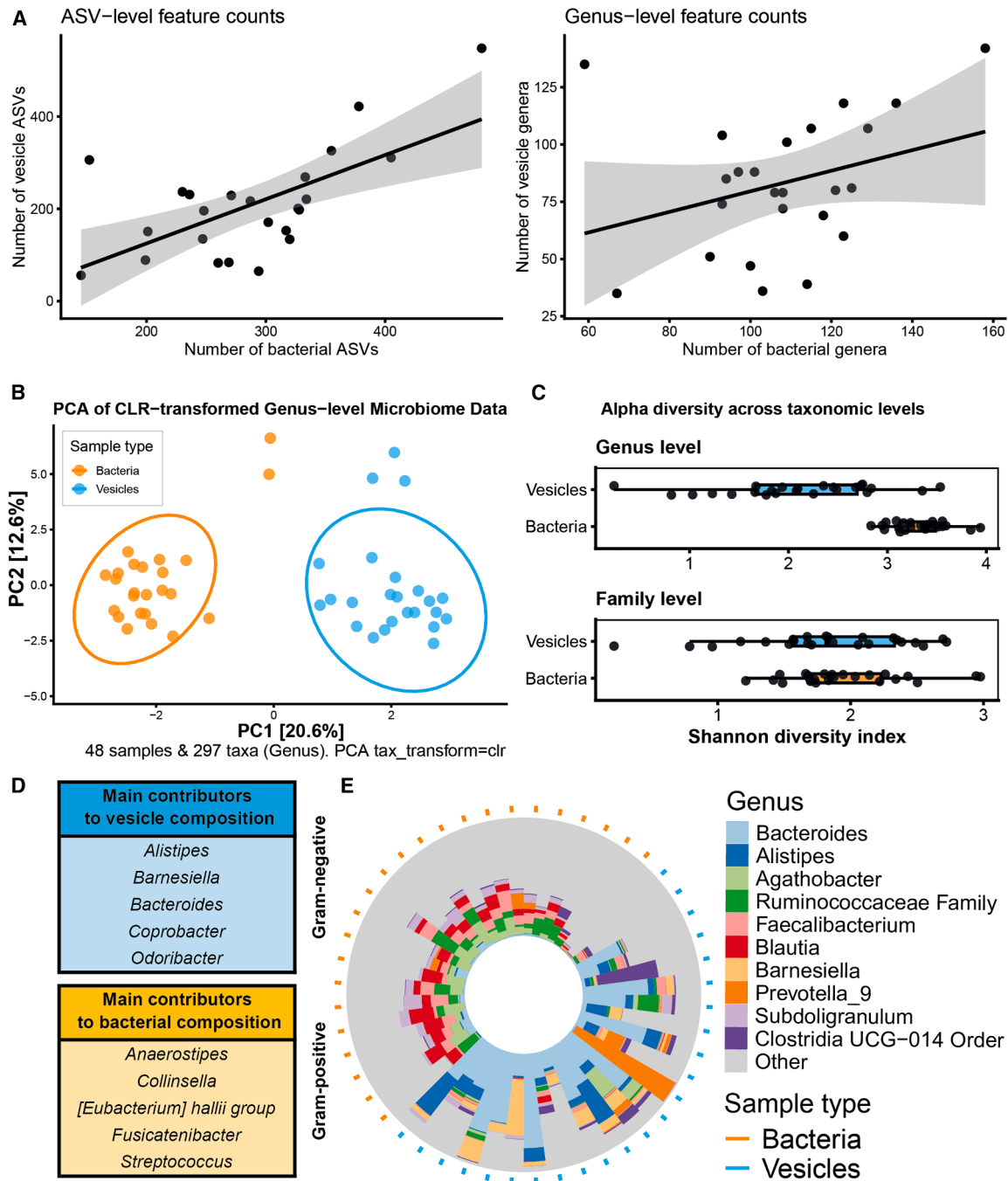


**Figure 1. Vesicle repertoires ( $n = 24$ ) characterized by 16S rRNA amplicon sequencing differ in composition from the bacterial compositions ( $n = 24$ ) that produced them**

(A) Linear relationships between the number of features (amplicon sequence variants/ASVs or Genera) detected in vesicle samples and the bacteria that produced them. Depicted are ordinary least squares linear regressions with 95% confidence intervals. For ASVs,  $p = 0.0098$  ( $R^2 = 0.41$ ), for Genera,  $p = 0.11$  ( $R^2 = 0.10$ ).

(B) Principal component analysis (PCA) of CLR-transformed genus-level compositions (vesicles vs. bacteria). Aitchison distance PERMANOVA  $p < 0.001$ .

(C) Shannon diversity of bacterial and vesicle compositions at the genus and family levels. Boxplots compare bacteria and vesicles; Wilcoxon rank-sum test was performed at genus ( $p = 2.7 \times 10^{-9}$ ) and family ( $p = 0.574$ ). Boxes represent the interquartile range, and whiskers extend to 1.5x the interquartile range.

(D) Top 5 most discriminative taxa for vesicle and bacterial compositions at the genus taxonomic level.

(E) Iris plot displays the most prevalent taxa constituting vesicle or bacterial compositions. Compositions are grouped together based on similarity.

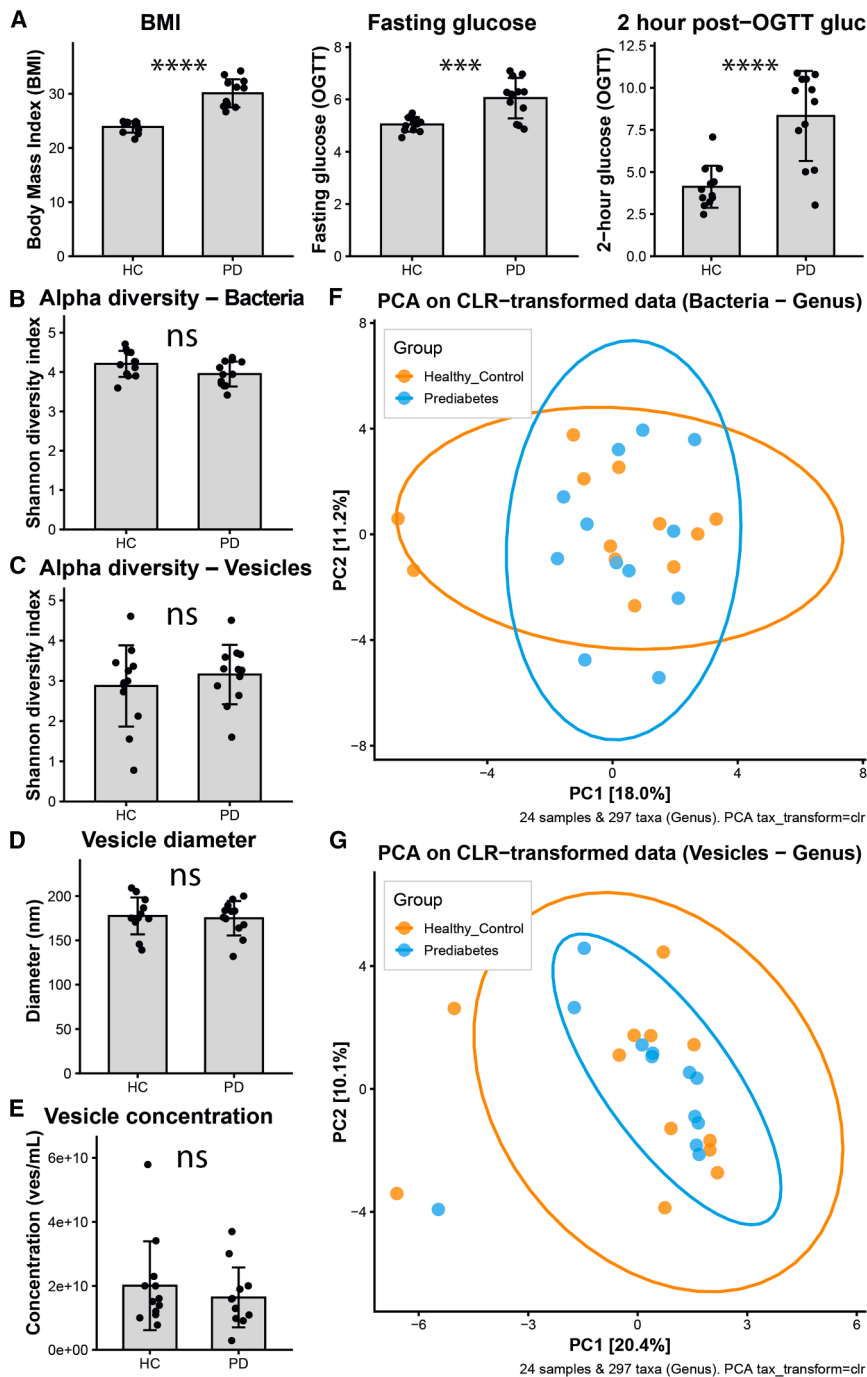


**Figure 2. No compositional differences in bacteria or vesicles between distinct metabolic phenotypes**

(A) Metabolic parameters, BMI, fasting plasma glucose levels, and plasma glucose levels 2 h post OGTT are elevated in PD.

(B) No differences in bacterial compositional richness between groups.

(C) No differences in vesicle compositional richness between groups.

(D) No differences in mean vesicle size between groups.

(E) No differences in mean vesicle concentration between groups.

(A–E) Bars represent mean  $\pm$  standard deviation. Statistical testing of single-variable data was performed using unpaired two-tailed t-testing. Significance levels are indicated as \*\*\* $p < 0.001$ , \*\*\*\* $p < 0.0001$ , ns; not significant.

(F) Principal component analysis (PCA) of CLR-transformed genus-level bacterial compositions (HC vs. PD). Aitchison distance PERMANOVA  $p = 0.47$ .

(G) Principal component analysis (PCA) of CLR-transformed genus-level vesicle compositions (HC vs. PD). Aitchison distance PERMANOVA  $p = 0.879$ . BMI: body mass index in  $\text{kg}/\text{m}^2$ . OGTT: oral glucose tolerance test. HC: healthy control. PD: prediabetes.

antigens and proteases.<sup>14,25</sup> Vesicle-mediated transport of such bacterial products has been found to be able to disturb normal gut barrier function.<sup>26,27</sup>

With respect to non-communicable diseases such as (pre)diabetes and obesity, the pathophysiological role of gut-derived bMVs is not well understood. Although researchers have reported certain bacterial taxa to be more abundant than others in metabolic disease, causal relationships between the presence/abundance of such taxa and their vesicles in pathophysiology are not well defined. For example, an increase in the ratio between two prominent bacterial phyla, Firmicutes (Bacillota) and Bacteroidetes (Bacteroidota) (F/B ratio) has been reported in obesity,<sup>28,29</sup> although there is no definitive agreement on this paradigm.<sup>30</sup> Beyond phyla-level resolution,

however, a consistent finding is that butyrate-producing genera are reduced, illustrating that analyses at deeper taxonomic levels are required.<sup>31</sup> Various strategies exist to improve host (metabolic) health through the modulation of gut microbiota, such as probiotics, prebiotics, postbiotics, and fecal microbiota transplantation (FMT).<sup>32</sup> Such interventions aim to establish a more diverse, less inflammatory microbiome that is more proficient at producing SCFAs, for example. However, defining a healthy microbiome and properly understanding

host cells, facilitates delivery to, for example, Toll-like receptor 9 (TLR9).<sup>20</sup> Other pathogen-recognition receptors that can be activated by bacterial membrane vesicles include TLR2, TLR4, TLR5, and cGAS.<sup>21,22</sup>

In complex ecosystems, bMVs are involved in bacteria-bacteria interactions (competitive or symbiotic) as well, and could therefore influence the bacterial composition of the gut microbiome itself.<sup>23,24</sup> Furthermore, these bMVs could modulate mucosal immunity and inflammation by transporting bacterial

**Table 1. Baseline study population characteristics**

	HC group (n=12) Mean (SD)	PD group (n=12) Mean (SD)	p-value
BMI (kg/m <sup>2</sup> )	23.9 (1)	30.09 (2.5)	<0.0001
Age (yrs)	53.7 (12)	59.3 (6.5)	0.18
Weight (kg)	76.8 (6.4)	97.3 (9.6)	<0.0001
Length (cm)	179 (5.9)	180 (6.3)	0.85
WH_ratio	0.92 (0.04)	1.01 (0.05)	<0.001
Fasting gluc (mM)	5.0 (0.3)	6.1 (0.7)	<0.001
2h gluc OGTT (mM)	4.1 (1.2)	8.3 (2.6)	<0.0001

Unpaired student's *t* test used for significance index.

BMI, Body mass index; OGTT, Oral glucose tolerance test.

microbiota-host interactions in human metabolic health necessitates the identification of all relevant communication pathways between bacteria and their host.

Studying gut-bacteria-derived bMVs, as a proxy of gut bacterial activity rather than solely their presence, could help explain metabolic disease pathophysiology. Importantly, research linking gut bacteria (and their metabolites/vesicles) to host metabolism often focuses on individual taxa of interest, whose abundance can be correlated to a phenotype or outcome.<sup>11</sup> For example, *Akkermansia muciniphila*, one of the hundreds of different bacterial species inhabiting the mammalian gut, has been found to produce bMVs that protect mice from high-fat diet-induced obesity.<sup>33</sup> Intestinal inflammation, a hallmark of obesity,<sup>34,35</sup> was previously reported to be reduced through the release of vesicles by *Bacteroides fragilis*.<sup>36,37</sup> Such examples illustrate how, in a particular setting, single bacterial taxa could have a significant influence on host health through the production of bacterial membrane vesicles.

We aim to investigate the composition and functionality of gut bacteria and their vesicles in the context of prediabetes, to uncover mechanisms through which the microbiome could contribute to the pathophysiology of human metabolic disease. To this end, we characterize the feces-derived bacterial membrane vesicle repertoire alongside its bacterial microbiome in study participants with prediabetes and healthy controls. In addition, we use an established *in vitro* human macrophage cell model to determine immunological properties of feces-derived vesicles in both groups.

## RESULTS

### Bacterial compositions differ from vesicle compositions

In general, the number of different bacterial amplicon sequence variants (ASVs) detected in a fecal sample correlates positively with the number of different vesicle ASVs detected in that sample (Figure 1A). This suggests that a larger number of distinct types of bacteria produce a larger number of distinct types of vesicles. Furthermore, Principal component-based composition analysis demonstrates highly distinct clustering between vesicle and bacterial DNA (Figure 1B). Intriguingly, on average the alpha diversity of vesicle compositions is lower than that of bacterial compositions, further suggesting that, in a given bacterial popu-

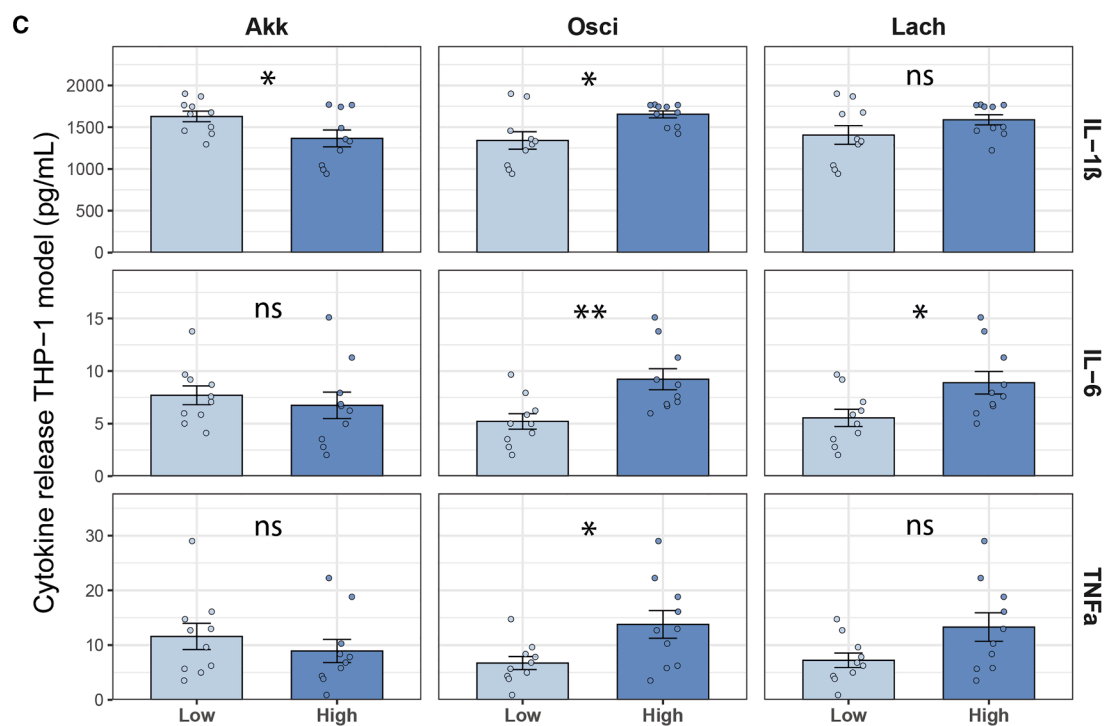
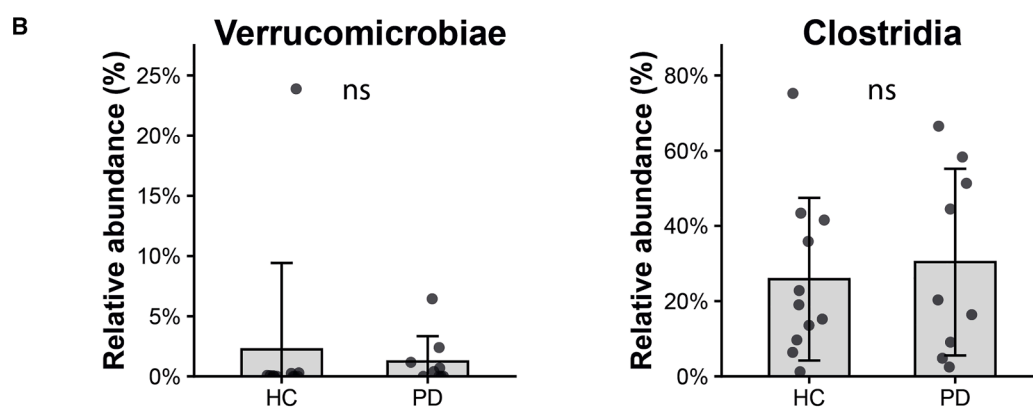
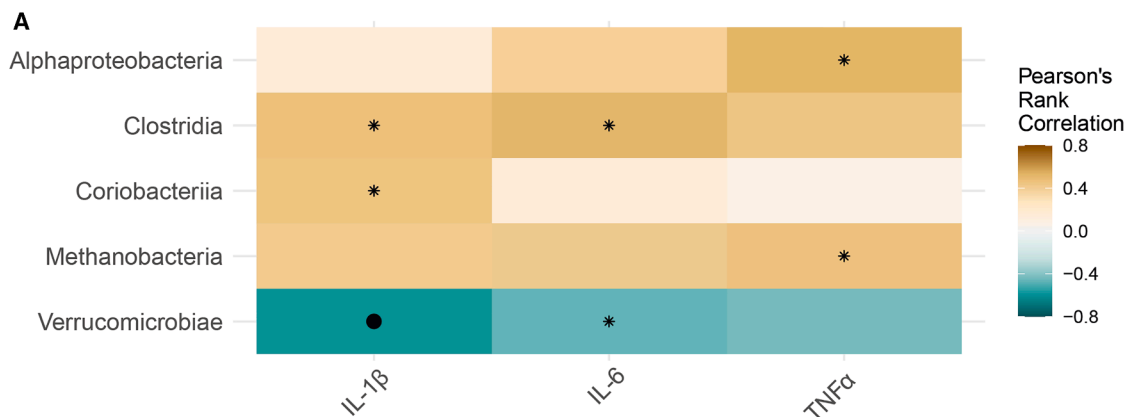
lation occupying a niche, not all bacteria appear to contribute to bMV production to an equal extent (Figure 1C). The main taxa constituting the vesicle and bacterial compositions, however, are vastly different. Gram-negative taxa, including *Alistipes* and *Barnesiella*, are overrepresented in vesicle repertoires while Gram-positive taxa, such as *Anaerostipes* and *Collinsella*, are overrepresented at the bacterial level (Figure 1D). In summary, the composition of feces-derived bacterial membrane vesicles is vastly different from the composition of their bacterial producer strains in terms of the 16S rDNA repertoire (Figure 1E).

### No differences in bacterial or vesicle compositions between participant groups

Participants in the prediabetes (PD) group were characterized by elevated BMI, increased fasting plasma glucose levels, and increased plasma glucose levels 2 h post-OGTT compared to HC participants (Figure 2A and Table 1). Between phenotypes, no differences were observed in alpha diversity of bacteria (Figure 2B) or vesicles (Figure 2C). Moreover, no differences in mean vesicle size (Figure 2D) or mean vesicle concentrations (Figure 2E) were observed between groups. Further grouping of participants with respect to fasting glucose and glucose tolerance did not indicate differences stratified by DNA compositions (Table S1). In comparing overall bacterial (Figure 2F) or overall vesicle (Figure 2G) compositions using principal component analysis, no distinct clustering was observed between phenotypes.

### Vesicle-associated DNA predicts inflammatory potential

While no overall compositional differences were observed between participant groups, the abundance of certain taxa was correlated with the inflammatory properties of normalized vesicle repertoires. At the class level, regression analysis indicated that the proportional abundance of Verrucomicrobiae inversely correlated with inflammatory markers IL-1 $\beta$  and IL-6, which were produced by THP-1 macrophages in response to exposure to normalized vesicle amounts. While not reaching statistical significance following FDR correction, the opposite was observed for Clostridia abundance (Figures 3A and S2). No differential abundances of these bacterial classes could be observed between participant phenotypes at the class level (Figure 3B) or lower taxonomic levels within these classes (data not shown). The bacterial compositions (Figure S3) and the absolute amount of vesicle-associated DNA (Figure S4) were poor predictors of vesicle-induced inflammation. In order to further investigate the relationship between vesicle composition and function, we stratified vesicle repertoires 50/50 by the abundance of the DNA from the taxa of interest (e.g., 50% of samples with the lowest relative abundance of a taxon vs. 50% of samples with the highest relative abundance of this taxon). The main Verrucomicrobiae anti-inflammatory driver belonged to the Akkermansiaceae family and the main Clostridia proinflammatory drivers belong to the Oscillospiraceae and Lachnospiraceae families. The 50% of vesicle repertoires characterized by the lowest proportional abundance of Akkermansiaceae induced significantly more IL-1 $\beta$  in our THP-1 model, and the same trend can be observed for IL-6 and TNF $\alpha$ . For Oscillospiraceae and Lachnospiraceae, the opposite can be observed, with more inflammatory cytokine



(legend on next page)

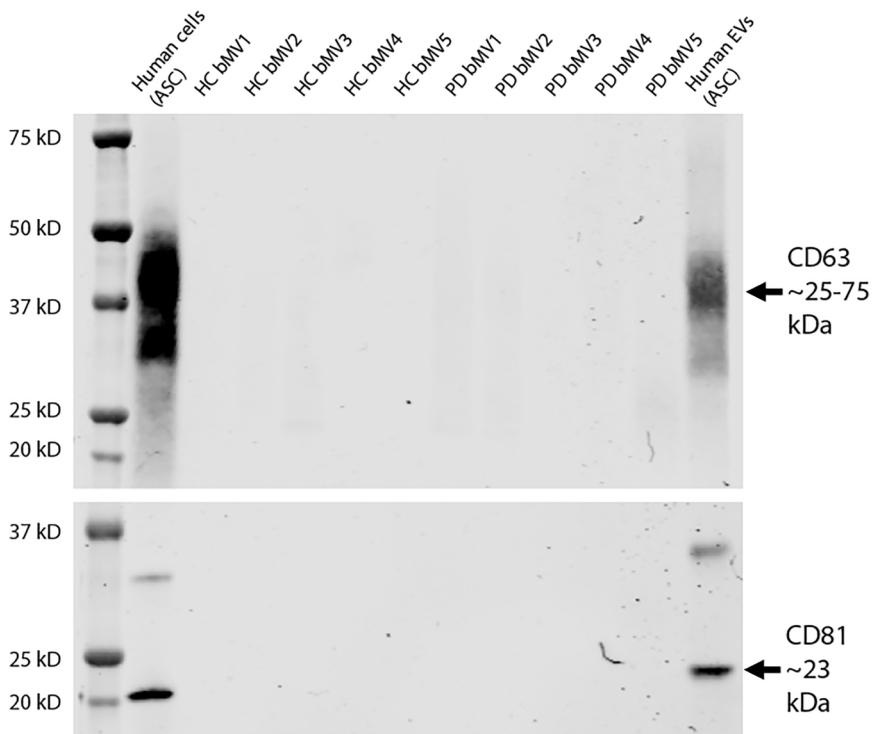


**Figure 4. Western blot analysis of classical eukaryotic vesicle markers CD63 and CD81**

To determine the contamination of gut-derived bMV repertoires by human host extracellular vesicles (EVs), detection of the human EV markers CD63 and CD81 was performed on bMV samples. As positive controls for the used antibodies, primary Adipocyte stem cell lysate, and its separated EVs were included. Eukaryotic EV markers were positive in the control samples only.

directly mirror the bacterial communities by which they were produced. Certain bacterial taxa were found to contribute disproportionately to bMV DNA, although in general, an increased richness in bacteria followed an increased richness in bMV DNA. Interestingly, the proportion of DNA from Gram-negative bacteria was much higher at the vesicle level. This suggests that bMV composition might be a function of not only bacterial presence but also their inherent biology (i.e., cell wall composition), or a consequence of Gram-negative bacteria more readily “loading” bMVs with their DNA.

release induced by the 50% of vesicle repertoires richest in these Clostridia DNA signatures (Figure 3C).

**Isolated bacterial membrane vesicle repertoires are characterized by a negligible presence of host-derived vesicle signatures**

Western blot analyses showed no marked differences in the presence of contaminating host extracellular vesicles (as determined by the presence of typical eukaryotic extracellular vesicle markers CD63 and CD81) (Figures 4 and S5–S7). Furthermore, OmpA, a marker for Gram-negative bacteria, was detectable in bMV repertoires but not in host cells or their derived EVs (Figures 5 and S8).

**DISCUSSION**

This study aimed to investigate the nature and properties of gut-derived bacterial membrane vesicles (bMVs) in individuals with prediabetes. Our results reveal significant complexity in the relationship between gut microbiota, bMV production, and host (metabolic) responses. One of the key findings of this study was that the DNA composition of gut-derived bMVs did not

Gram-positive bacteria, which lack an outer membrane and have a thicker peptidoglycan layer,<sup>14</sup> appear to be less prominent contributors to bMV repertoires in our study. The first described bacterial membrane vesicles, termed outer membrane vesicles (OMVs), were indeed derived from Gram-negative bacteria.<sup>10,38</sup> The unique structural architecture of the Gram-negative bacterial cell envelope herein facilitates the formation of these OMVs, as it is characterized by an inner and outer membrane, separated by a periplasmic space.<sup>38</sup> Small portions of the outer membrane can be pinched off to form an OMV.<sup>14</sup> In line with our results, the formation of Gram-positive bacteria-derived bMVs appears rarer. Vesiculation by Gram-positive bacteria has been described as a consequence of bacterial cell death, but also as a result of endolysin-induced protrusion of the cytoplasmic membrane through the peptidoglycan layer.<sup>14,39</sup> The cytoplasmic membrane material can herein be released into the extracellular milieu as bMVs.<sup>40</sup> Discovered later and less studied, bMVs derived from Gram-positive bacteria appear to be less ubiquitous than Gram-negative bMVs. Electron microscopic imaging of purified bMV samples allows the observation of nanosized vesicles (Figures 6 and 7). Cryogenically prepared samples can even be observed with a corona of associated

**Figure 3. A: Vesicle composition by DNA determines inflammatory potential, but differences are not phenotype-specific**

(A) Pearson’s regression analyses overview at class taxonomic level indicating relative taxa abundances correlating positively (proinflammatory) and negatively (antiinflammatory) with outcome. Heatmap shows Spearman’s rank correlation coefficients. \**p* < 0.05, (uncorrected). Filled circles indicate significance after Benjamini-Hochberg false discovery rate correction, *q* < 0.05.

(B) Comparison of proportional abundance of taxa (class) constituting vesicle repertoires by phenotype group. Bars represent mean ± standard deviation.

(C) 50% highest-proportion (*n* = 10) vs. 50% lowest-proportion (*n* = 10) dichotomized comparison of cytokine induction by taxa of interest (family). Bars represent mean ± standard error of the mean. B and C: Statistical testing was performed using unpaired two-tailed t-testing. Significance levels are indicated \*\**p* < 0.01, \**p* < 0.05, ns; not significant. C: No FDR correction was performed in this specific design, as statistical analyses were hypothesis-driven and focused on a limited number of biologically pre-specified cytokines. HC: healthy control. PD: prediabetes.

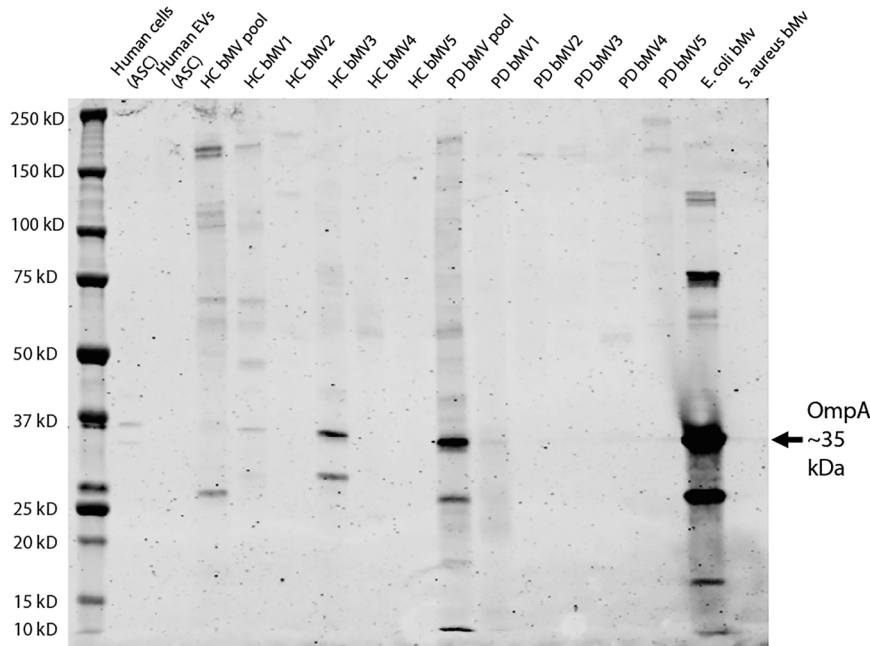


**Figure 5. Detectability of bacterial vesicle marker in gut-bMV repertoires**

Western blot analysis of *Escherichia coli* outer membrane protein A (OmpA). OmpA can be detected in some of the gut-bMV repertoires as vesicles by this taxon (family Enterobacteriaceae), which can contribute to vesicle production. OmpA was selected, given that no pan-bacterial vesicle marker is available. Positive control: *E. coli* K12 monoculture-derived vesicles. Negative control: *Staphylococcus aureus* monoculture-derived vesicles.

molecules, potentially indicating peptidoglycan or transmembrane proteins (Figure 6).

Importantly, with respect to participants with prediabetes (BMI >25 kg/m<sup>2</sup> and impaired fasting glucose and/or impaired glucose tolerance) and healthy controls (BMI <25 kg/m<sup>2</sup>, normoglycemic), we did not observe compositional differences in bacteria or bMVs, nor differences in vesicle characteristics isolated from fecal samples. Here, it should be noted that the currently studied population was relatively small and study participants did not exhibit extreme phenotypic traits or comorbidities as seen in type 2 diabetes and (morbid) obesity. Instead, data reflect continuous relationships and not group-based differences.

In obesity and type 2 diabetes, bacterial compositions are often found to be less diverse,<sup>41,42</sup> and can be characterized by outgrowth of opportunistic taxa such as *Blautia* and *Ruminococcus* (fam. Lachnospiraceae)<sup>43,44</sup> at the cost of bacterial taxa often perceived as benign, such as *Akkermansia* and *Bifidobacterium*.<sup>44–47</sup> Once more, bacterial composition analysis might only reflect bacterial presence rather than activity, while analyzing vesicles allows insights into bacterium-host or bacterium-bacterium interactions in disease. Indicatively, feces-derived bMV repertoires were previously identified as a more effective differentiation marker between healthy controls and patients with IBD than stool bacteria themselves.<sup>48</sup> This suggests that bMV production reflects a degree of bacterial activity and functionalities not fully capturable by the compositional analysis of gut bacteria alone.

Moreover, bMVs have been found capable of crossing epithelial barriers, either through translocation facilitated by their small size,<sup>49,50</sup> or through the disruption of barrier integrity.<sup>26,50</sup> In animal studies, such translocations of gut microbiota-produced bMVs from the intestinal lumen into systemic circulation have previously been described.<sup>51–53</sup> In these studies, homing of

bMVs to distant host organs induced localized inflammation and altered host energy metabolism.<sup>53</sup> Diabetic phenotypes were, for example, observed following the translocation of *Pseudomonas panacis* vesicles originating from the gastrointestinal tract to systemic circulation in mice.<sup>53</sup> In humans, effects on host metabolism or tissue inflammation resulting from the translocation of spe-

cific microbiota-derived bMVs have not yet been documented. However, the translocation of gut-luminal content due to compromised gut barrier integrity has been described in IBD,<sup>54</sup> HIV,<sup>55</sup> aging,<sup>56</sup> and alcohol consumption.<sup>57</sup> As such, further research on gut bacterial signatures such as bMVs in systemic circulation in the context of human metabolic disease is urgently warranted.

Given that feces-derived bMVs carry bacterial immunogenic signatures such as LPS,<sup>53,58</sup> LTA,<sup>53</sup> or outer membrane proteins,<sup>59</sup> we sought to compare the inflammatory potentials of the bMV repertoires obtained from our study participants *in vitro*, given that a low-grade systemic inflammation caused by circulating bacterial endotoxins is described in human metabolic disease.<sup>35</sup> The *in vitro* use of human macrophage cultures has been an effective way to investigate the biological effects of bMVs on human cells.<sup>60</sup> In this study, it enabled the characterization of their inflammatory potential to reveal substantial differences between vesicle repertoires. However, given the large within-group variation, no significant differences between phenotypes could be detected in the population studied. It has been reported previously that extracellular vesicles of host/eukaryotic origin can contaminate feces-derived vesicle repertoires,<sup>61</sup> and as such, vesicle count data can be skewed by the presence of these particles. Nevertheless, the presence of host-EV-derived membrane markers could not be demonstrated in our bMV repertoires (Figure 4), while the presence of an Enterobacteriaceae membrane marker, OmpA, could be indicated (Figure 5). In previous work by our group, the contaminating presence of host-EVs in bMV repertoires was indeed found to be minor.<sup>60</sup>

Our results indicate that bMVs rich in DNA from Gram-positive taxa such as Oscillospiraceae and Lachnospiraceae, induced more pronounced inflammatory responses in these cells, while bMVs rich in Gram-negative Akkermansiaceae DNA induced

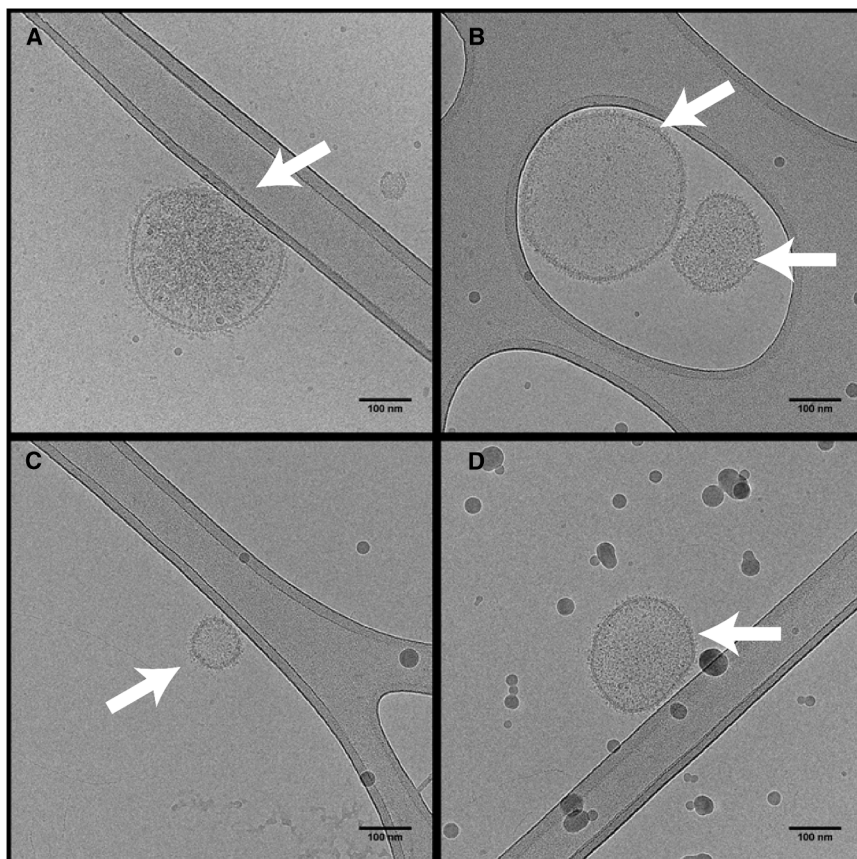


**Figure 6. CryoTEM images (200 kV) of gut-bacteria derived membrane vesicles analyzed in this study**

(A–D) Arrows indicate spherical nanosized bMVs enclosed by a lipid bilayer. Scale-bars denote 100 nm.

betes and obesity. Studying bMVs in gut-host communications may lead to the expansion of biomarkers for metabolic diseases, and opens avenues for therapeutic modulation through, for example, probiotics, prebiotics, and postbiotics.

#### Limitations of the study

This study reports on the *ex vivo* characterization of feces-derived bacterial membrane vesicles (bMVs), which were used to stimulate *in vitro* differentiated THP-1 macrophages. One of the main findings is that DNA-determined compositionality is a predictor for the inflammatory potential of bMVs, with potential relevance for gut- and metabolic health. However, the gut microbiota and, inherently, also its vesicle production are highly dynamic, and cross-sectional analyses do not facilitate an understanding of the composition/functionality as it changes over time (influenced by e.g., diet, travel, and disease conditions). Furthermore,

statistical power in investigating phenotype-specific differences is limited because of the use of a relatively small number of study participants with prediabetes and overweight/obesity. Here, the investigation of more discordant phenotypes (e.g., study participants exhibiting type 2 diabetes and morbid obesity) could improve resolution.

#### RESOURCE AVAILABILITY

##### Lead contact

Requests for further information and resources should be directed to and will be fulfilled by the lead contact, Frank Stassen ([f.stassen@maastrichtuniversity.nl](mailto:f.stassen@maastrichtuniversity.nl)).

##### Materials availability

This study did not generate new unique reagents.

##### Data and code availability

16S rRNA gene sequencing data have been deposited at the European Nucleotide Archive repository under accession number PRJEB96207, and are publicly available as of the date of publication. This article does not report original code. Any additional information required to reanalyze the data reported in this article is available from the [lead contact](#) upon request.

#### ACKNOWLEDGMENTS

This research did not receive any specific grant from funding agencies in the public, commercial, or not-for-profit sectors. We thank H. Duimel and C. López Iglesias (Microscopy Core lab, Maastricht) for their valuable assistance in

less inflammatory responses. In humans, colonization with specific genera such as *Akkermansia* is generally perceived as benign, as the presence of these bacteria in the intestinal lumen of study participants and patients is concomitant with healthier metabolic outcomes such as reduced cholesterol levels and increased insulin sensitivity.<sup>62,63</sup> These observed differences in inflammatory responses suggest that specific bacterial taxa may have a greater impact on host metabolism and immune responses through bMV production and dissemination, as functional characteristics of bMVs are derived from their parent bacteria. This implies that targeting specific microbial species or their vesiculation may offer a therapeutic strategy for modulating inflammation and improving metabolic health. However, the precise mechanisms inducing gut-microbial vesiculation and those by which bMVs influence host metabolism, remain to be further elucidated.

In summary, individuals with prediabetes showed no significant differences in gut bacterial or vesicle composition compared with healthy controls. Nevertheless, these bMVs displayed distinct inflammatory properties *ex vivo*. The use of marker-gene sequencing in characterizing the bacterial origins of bMV repertoires herein allows an extra perspective on microbiome-host interactions, as these bMVs mediate microbiological activity. Understanding the complex interplay between gut microbiota, host metabolism, and health is crucial in addressing the rising global prevalence of metabolic disorders such as dia-

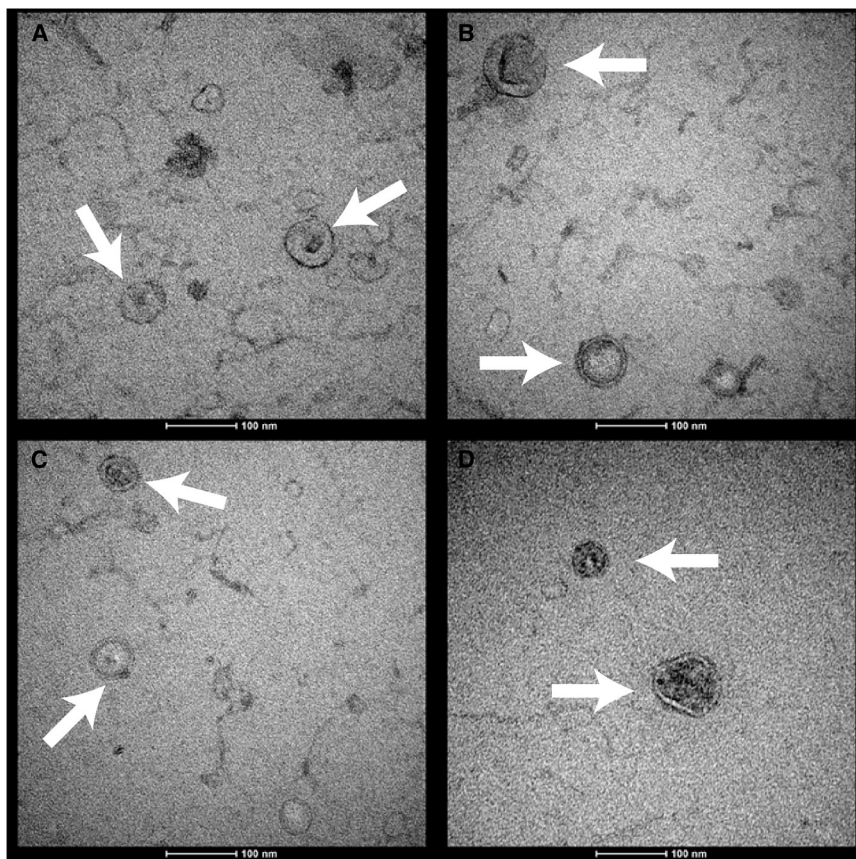


**Figure 7. Room temperature negative staining TEM images (120 kV) of gut-bacteria-derived membrane vesicles analyzed in this study**

(A–D) White arrows indicate bMVs contrasted by uranyl-salt deposition on the surface or borders of the vesicles. Scale-bars denote 100 nm.

generating transmission-electron microscopic images. The graphical abstract was created using [BioRender.com](https://www.bio-render.com/).

#### AUTHOR CONTRIBUTIONS

J.V. performed vesicle isolation, all characterizations, and wrote the article. L.M. performed western blotting experiments and wrote the methods and results sections on these experiments. E.C. collected anthropometric data. J.J. and F.S. provided technical support. J.J., E.C., E.B., P.S., and F.S. facilitated the conceptualization and execution of the work. All authors critically reviewed and revised the article and agree with its submission.

#### DECLARATION OF INTERESTS

The authors declare no competing interests.

#### STAR★METHODS

Detailed methods are provided in the online version of this paper and include the following:

- [KEY RESOURCES TABLE](#)
- [EXPERIMENTAL MODEL AND STUDY PARTICIPANT DETAILS](#)
  - Human subjects
  - Cell-lines
- [METHOD DETAILS](#)
  - Fecal bacterial DNA extraction
  - Bacterial membrane vesicle isolation and purification
  - Nanoparticle tracking analysis
  - Western blot analysis

- Negative-staining transmission electron microscopy
- Cryo-transmission electron microscopy
- 16S rRNA gene amplification and sequencing
- Cell culture stimulation and harvest
- Cytokine ELISA
- [QUANTIFICATION AND STATISTICAL ANALYSIS](#)
  - Sequencing data processing
  - Statistical analysis

#### SUPPLEMENTAL INFORMATION

Supplemental information can be found online at <https://doi.org/10.1016/j.isci.2026.115088>.

Received: August 21, 2025

Revised: December 19, 2025

Accepted: February 16, 2026

Published: February 19, 2026

#### REFERENCES

1. Joos, R., Boucher, K., Lavelle, A., Arumugam, M., Blaser, M.J., Claesson, M.J., Clarke, G., Cotter, P.D., De Sordi, L., Dominguez-Bello, M.G., et al. (2025). Examining the healthy human microbiome concept. *Nat. Rev. Microbiol.* 23, 192–205. <https://doi.org/10.1038/s41579-024-01107-0>.
2. Canfora, E.E., Jocken, J.W., and Blaak, E.E. (2015). Short-chain fatty acids in control of body weight and insulin sensitivity. *Nat. Rev. Endocrinol.* 11, 577–591. <https://doi.org/10.1038/nrendo.2015.128>.

3. Ansaldo, E., Farley, T.K., and Belkaid, Y. (2021). Control of immunity by the microbiota. *Annu. Rev. Immunol.* **39**, 449–479. <https://doi.org/10.1146/annurev-immunol-093019-112348>.
4. Delzenne, N.M., Bindels, L.B., Neyrinck, A.M., and Walter, J. (2025). The gut microbiome and dietary fibres: implications in obesity, cardiometabolic diseases and cancer. *Nat. Rev. Microbiol.* **23**, 225–238. <https://doi.org/10.1038/s41579-024-01108-z>.
5. Xie, H., Yu, S., Tang, M., Xun, Y., Shen, Q., and Wu, G. (2025). Gut microbiota dysbiosis in inflammatory bowel disease: interaction with intestinal barriers and microbiota-targeted treatment options. *Front. Cell. Infect. Microbiol.* **15**, 1608025. <https://doi.org/10.3389/fcimb.2025.1608025>.
6. Kumari, S., Desai, V., Sivakumar, S., Sikri, K., and Kumar, M. (2025). Association between gut microbial dysbiosis and Alzheimer's disease: an umbrella review. *npj Dementia* **1**, 41. <https://doi.org/10.1038/s44400-025-00048-6>.
7. Amabebe, E., Robert, F.O., Agbalalah, T., and Orubu, E.S.F. (2020). Microbial dysbiosis-induced obesity: role of gut microbiota in homeostasis of energy metabolism. *Br. J. Nutr.* **123**, 1127–1137. <https://doi.org/10.1017/S0007114520000380>.
8. Bielka, W., Przekaz, A., and Pawlik, A. (2022). The role of the gut microbiota in the pathogenesis of diabetes. *Int. J. Mol. Sci.* **23**, 480. <https://doi.org/10.3390/ijms23010480>.
9. Canfora, E.E., Hermes, G.D.A., Müller, M., Bastings, J., Vaughan, E.E., van Den Berg, M.A., Holst, J.J., Venema, K., Zoetendal, E.G., and Blaak, E.E. (2022). Fiber mixture-specific effect on distal colonic fermentation and metabolic health in lean but not in prediabetic men. *Gut Microbes* **14**, 2009297. <https://doi.org/10.1080/19490976.2021.2009297>.
10. Diaz-Garrido, N., Badia, J., and Baldomà, L. (2021). Microbiota-derived extracellular vesicles in interkingdom communication in the gut. *J. Extracell. Vesicles* **10**, e12161. <https://doi.org/10.1002/jev2.12161>.
11. Verbunt, J., Jocken, J., Blaak, E., Savelkoul, P., and Stassen, F. (2024). Gut-bacteria derived membrane vesicles and host metabolic health: a narrative review. *Gut Microbes* **16**, 2359515. <https://doi.org/10.1080/19490976.2024.2359515>.
12. Volgers, C., Savelkoul, P.H.M., and Stassen, F.R.M. (2018). Gram-negative bacterial membrane vesicle release in response to the host-environment: different threats, same trick? *Crit. Rev. Microbiol.* **44**, 258–273. <https://doi.org/10.1080/1040841X.2017.1353949>.
13. Abraham, L., Raise, A., Beney, L., Lapaquette, P., and Rieu, A. (2025). Membrane vesicles produced by next-generation probiotics from the gut as innovative tools for human health. *Gut Microbes* **17**, 2552344. <https://doi.org/10.1080/19490976.2025.2552344>.
14. Toyofuku, M., Schild, S., Kaparakis-Liaskos, M., and Eberl, L. (2023). Composition and functions of bacterial membrane vesicles. *Nat. Rev. Microbiol.* **21**, 415–430. <https://doi.org/10.1038/s41579-023-00875-5>.
15. Mottawea, W., Yousuf, B., Sultan, S., Ahmed, T., Yeo, J., Hüttmann, N., Li, Y., Bouhlef, N.E., Hassan, H., Zhang, X., et al. (2025). Multi-level analysis of gut microbiome extracellular vesicles-host interaction reveals a connection to gut-brain axis signaling. *Microbiol. Spectr.* **13**, e0136824. <https://doi.org/10.1128/spectrum.01368-24>.
16. Kaisanlahti, A., Turunen, J., Hekkala, J., Mishra, S., Karikka, S., Amatya, S.B., Paalanne, N., Kruger, J., Portaankorva, A.M., Koivunen, J., et al. (2025). Gut microbiota-derived extracellular vesicles form a distinct entity from gut microbiota. *mSystems* **10**, e0031125. <https://doi.org/10.1128/mSystems.00311-25>.
17. Bielaszewska, M., Daniel, O., Karch, H., and Mellmann, A. (2020). Dissemination of the bla CTX-M-15 gene among Enterobacteriaceae via outer membrane vesicles. *J. Antimicrob. Chemother.* **75**, 2442–2451. <https://doi.org/10.1093/jac/dkaa214>.
18. Wen, M., Wang, J., Ou, Z., Nie, G., Chen, Y., Li, M., Wu, Z., Xiong, S., Zhou, H., Yang, Z., et al. (2023). Bacterial extracellular vesicles: A position paper by the microbial vesicles task force of the Chinese society for extracellular vesicles. *Interdisciplinary Medicine* **1**, e20230017.
19. Shen, Z., Qin, J., Xiang, G., Chen, T., Nurxat, N., Gao, Q., Wang, C., Zhang, H., Liu, Y., and Li, M. (2024). Outer membrane vesicles mediating horizontal transfer of the epidemic bla OXA-232 carbapenemase gene among Enterobacterales. *Emerg. Microbes Infect.* **13**, 2290840. <https://doi.org/10.1080/22221751.2023.2290840>.
20. Bitto, N.J., Chapman, R., Pidot, S., Costin, A., Lo, C., Choi, J., D'Cruze, T., Reynolds, E.C., Dashper, S.G., Turnbull, L., et al. (2017). Bacterial membrane vesicles transport their DNA cargo into host cells. *Sci. Rep.* **7**, 7072. <https://doi.org/10.1038/s41598-017-07288-4>.
21. Balhuizen, M.D., Versluis, C.M., van Grondelle, M.O., Veldhuizen, E.J.A., and Haagsman, H.P. (2022). Modulation of outer membrane vesicle-based immune responses by cathelicidins. *Vaccine* **40**, 2399–2408. <https://doi.org/10.1016/j.vaccine.2022.03.015>.
22. Erttmann, S.F., Swacha, P., Aung, K.M., Brinddefalk, B., Jiang, H., Härtlova, A., Uhlin, B.E., Wai, S.N., and Gekara, N.O. (2022). The gut microbiota prime systemic antiviral immunity via the cGAS-STING-IFN-I axis. *Immunity* **55**, 847–861.e10. <https://doi.org/10.1016/j.immuni.2022.04.006>.
23. Lee, E.Y., Bang, J.Y., Park, G.W., Choi, D.S., Kang, J.S., Kim, H.J., Park, K.S., Lee, J.O., Kim, Y.K., Kwon, K.H., et al. (2007). Global proteomic profiling of native outer membrane vesicles derived from *Escherichia coli*. *Proteomics* **7**, 3143–3153. <https://doi.org/10.1002/pmic.200700196>.
24. Evans, A.G.L., Davey, H.M., Cookson, A., Currinn, H., Cooke-Fox, G., Stanczyk, P.J., and Whitworth, D.E. (2012). Predatory activity of *Myxococcus xanthus* outer-membrane vesicles and properties of their hydrolase cargo. *Microbiology* **158**, 2742–2752. <https://doi.org/10.1099/mic.0.060343-0>.
25. Elhenawy, W., Debelyy, M.O., and Feldman, M.F. (2014). Preferential packing of acidic glycosidases and proteases into *Bacteroides* outer membrane vesicles. *mBio* **5**, e00909–e00914. <https://doi.org/10.1128/mBio.00909-14>.
26. Cheng, W.T., Kantilal, H.K., and Davamani, F. (2020). The mechanism of *Bacteroides fragilis* toxin contributes to colon cancer formation. *Malays. J. Med. Sci.* **27**, 9–21. <https://doi.org/10.21315/mjms2020.27.4.2>.
27. Wick, E.C., Rabizadeh, S., Albesiano, E., Wu, X., Wu, S., Chan, J., Rhee, K.J., Ortega, G., Huso, D.L., Pardoll, D., et al. (2014). Stat3 activation in murine colitis induced by enterotoxigenic *Bacteroides fragilis*. *Inflamm. Bowel Dis.* **20**, 821–834. <https://doi.org/10.1097/MIB.0000000000000019>.
28. Musso, G., Gambino, R., and Cassader, M. (2010). Obesity, diabetes, and gut microbiota: the hygiene hypothesis expanded? *Diabetes Care* **33**, 2277–2284. <https://doi.org/10.2337/dc10-0556>.
29. Ley, R.E., Turnbaugh, P.J., Klein, S., and Gordon, J.I. (2006). Human gut microbes associated with obesity. *nature* **444**, 1022–1023. <https://doi.org/10.1038/4441022a>.
30. Magne, F., Gotteland, M., Gauthier, L., Zazueta, A., Pesoa, S., Navarrete, P., and Balamurugan, R. (2020). The firmicutes/bacteroidetes ratio: a relevant marker of gut dysbiosis in obese patients? *Nutrients* **12**, 1474. <https://doi.org/10.3390/nu12051474>.
31. Khan, M.T., Nieuwdorp, M., and Bäckhed, F. (2014). Microbial modulation of insulin sensitivity. *Cell Metab.* **20**, 753–760. <https://doi.org/10.1016/j.cmet.2014.07.006>.
32. Hou, S., Yu, J., Li, Y., Zhao, D., and Zhang, Z. (2025). Advances in Fecal Microbiota Transplantation for Gut Dysbiosis-Related Diseases. *Adv. Sci.* **12**, 2413197. <https://doi.org/10.1002/adv.202413197>.
33. Ashrafian, F., Keshavarz Azizi Raftar, S., Lari, A., Shahyari, A., Abdollahiyan, S., Moradi, H.R., Masoumi, M., Davari, M., Khatami, S., Omrani, M.D., et al. (2021). Extracellular vesicles and pasteurized cells derived from *Akkermansia muciniphila* protect against high-fat induced obesity

- in mice. *Microb. Cell Fact.* 20, 219. <https://doi.org/10.1186/s12934-021-01709-w>.
34. Rohm, T.V., Fuchs, R., Müller, R.L., Keller, L., Baumann, Z., Bosch, A.J.T., Schneider, R., Labes, D., Langer, I., Pilz, J.B., et al. (2021). Obesity in humans is characterized by gut inflammation as shown by pro-inflammatory intestinal macrophage accumulation. *Front. Immunol.* 12, 668654. <https://doi.org/10.3389/fimmu.2021.668654>.
  35. Chen, B., and Gautron, L. (2025). Gut-derived lipopolysaccharides and metabolic endotoxemia: a critical review. *Am. J. Physiol. Endocrinol. Metab.* 329, E746–E754. <https://doi.org/10.1152/ajpendo.00355.2025>.
  36. Shen, Y., Giardino Torchia, M.L., Lawson, G.W., Karp, C.L., Ashwell, J.D., and Mazmanian, S.K. (2012). Outer membrane vesicles of a human commensal mediate immune regulation and disease protection. *Cell Host Microbe* 12, 509–520. <https://doi.org/10.1016/j.chom.2012.08.004>.
  37. Chu, H., Khosravi, A., Kusumawardhani, I.P., Kwon, A.H.K., Vasconcelos, A.C., Cunha, L.D., Mayer, A.E., Shen, Y., Wu, W.L., Kambal, A., et al. (2016). Gene-microbiota interactions contribute to the pathogenesis of inflammatory bowel disease. *Science* 352, 1116–1120. <https://doi.org/10.1126/science.aad9948>.
  38. Kulp, A., and Kuehn, M.J. (2010). Biological functions and biogenesis of secreted bacterial outer membrane vesicles. *Annu. Rev. Microbiol.* 64, 163–184. <https://doi.org/10.1146/annurev.micro.091208.073413>.
  39. Dubey, G.P., Malli Mohan, G.B., Dubrovsky, A., Amen, T., Tsipshtein, S., Rouvinski, A., Rosenberg, A., Kaganovich, D., Sherman, E., Medalia, O., and Ben-Yehuda, S. (2016). Architecture and characteristics of bacterial nanotubes. *Dev. Cell* 36, 453–461. <https://doi.org/10.1016/j.devcel.2016.01.013>.
  40. Toyofuku, M., Cárcamo-Oyarce, G., Yamamoto, T., Eisenstein, F., Hsiao, C.C., Kurosawa, M., Gademann, K., Pilhofer, M., Nomura, N., and Eberl, L. (2017). Prophage-triggered membrane vesicle formation through peptidoglycan damage in *Bacillus subtilis*. *Nat. Commun.* 8, 481. <https://doi.org/10.1038/s41467-017-00492-w>.
  41. Zhou, Z., Sun, B., Yu, D., and Zhu, C. (2022). Gut microbiota: an important player in type 2 diabetes mellitus. *Front. Cell. Infect. Microbiol.* 12, 834485. <https://doi.org/10.3389/fcimb.2022.834485>.
  42. Scheithauer, T.P.M., Rampanelli, E., Nieuwdorp, M., Vallance, B.A., Verchere, C.B., van Raalte, D.H., and Herrema, H. (2020). Gut microbiota as a trigger for metabolic inflammation in obesity and type 2 diabetes. *Front. Immunol.* 11, 571731. <https://doi.org/10.3389/fimmu.2020.571731>.
  43. Dash, N.R., Al Bataineh, M.T., Alili, R., Al Safar, H., Alkhayyal, N., Prifti, E., Zucker, J.D., Belda, E., and Clément, K. (2023). Functional alterations and predictive capacity of gut microbiome in type 2 diabetes. *Sci. Rep.* 13, 22386. <https://doi.org/10.1038/s41598-023-49679-w>.
  44. Da Silva, C.C., Monteil, M.A., and Davis, E.M. (2020). Overweight and obesity in children are associated with an abundance of Firmicutes and reduction of Bifidobacterium in their gastrointestinal microbiota. *Child. Obes.* 16, 204–210. <https://doi.org/10.1089/chi.2019.0280>.
  45. Schneeberger, M., Everard, A., Gómez-Valadés, A.G., Matamoros, S., Ramírez, S., Delzenne, N.M., Gomis, R., Claret, M., and Cani, P.D. (2015). Akkermansia muciniphila inversely correlates with the onset of inflammation, altered adipose tissue metabolism and metabolic disorders during obesity in mice. *Sci. Rep.* 5, 16643. <https://doi.org/10.1038/srep16643>.
  46. Li, J., Yang, G., Zhang, Q., Liu, Z., Jiang, X., and Xin, Y. (2023). Function of Akkermansia muciniphila in type 2 diabetes and related diseases. *Front. Microbiol.* 14, 1172400. <https://doi.org/10.3389/fmicb.2023.1172400>.
  47. Dao, M.C., Everard, A., Aron-Wisniewsky, J., Sokolovska, N., Prifti, E., Vergier, E.O., Kayser, B.D., Levenez, F., Chilloux, J., Hoyle, L., et al. (2016). Akkermansia muciniphila and improved metabolic health during a dietary intervention in obesity: relationship with gut microbiome richness and ecology. *Gut* 65, 426–436. <https://doi.org/10.1136/gutjnl-2014-308778>.
  48. Heo, M., Park, Y.S., Yoon, H., Kim, N.E., Kim, K., Shin, C.M., Kim, N., and Lee, D.H. (2023). Potential of gut microbe-derived extracellular vesicles to differentiate inflammatory bowel disease patients from healthy controls. *Gut Liver* 17, 108–118. <https://doi.org/10.5009/gnl220081>.
  49. Chakaroun, R.M., Massier, L., and Kovacs, P. (2020). Gut microbiome, intestinal permeability, and tissue bacteria in metabolic disease: perpetrators or bystanders? *Nutrients* 12, 1082. <https://doi.org/10.3390/nu12041082>.
  50. Tulkens, J., Vergauwen, G., Van Deun, J., Geeurickx, E., Dhondt, B., Lippens, L., De Scheerder, M.A., Miinalainen, I., Rappu, P., De Geest, B.G., et al. (2020). Increased levels of systemic LPS-positive bacterial extracellular vesicles in patients with intestinal barrier dysfunction. *Gut* 69, 191–193. <https://doi.org/10.1136/gutjnl-2018-317726>.
  51. Bittel, M., Reichert, P., Sarfati, I., Dressel, A., Leikam, S., Uderhardt, S., Stolzer, I., Phu, T.A., Ng, M., Vu, N.K., et al. (2021). Visualizing transfer of microbial biomolecules by outer membrane vesicles in microbe-host-communication in vivo. *J. Extracell. Vesicles* 10, e12159. <https://doi.org/10.1002/jev2.12159>.
  52. Jones, E.J., Booth, C., Fonseca, S., Parker, A., Cross, K., Miquel-Clopés, A., Hautefort, I., Mayer, U., Wileman, T., Stentz, R., and Carding, S.R. (2020). The uptake, trafficking, and biodistribution of Bacteroides thetaio-taomicron generated outer membrane vesicles. *Front. Microbiol.* 11, 57. <https://doi.org/10.3389/fmicb.2020.00057>.
  53. Choi, Y., Kwon, Y., Kim, D.-K., Jeon, J., Jang, S.C., Wang, T., Ban, M., Kim, M.H., Jeon, S.G., Kim, M.S., et al. (2015). Gut microbe-derived extracellular vesicles induce insulin resistance, thereby impairing glucose metabolism in skeletal muscle. *Sci. Rep.* 5, 15878. <https://doi.org/10.1038/srep15878>.
  54. Chang, J., Leong, R.W., Wasinger, V.C., Ip, M., Yang, M., and Phan, T.G. (2017). Impaired intestinal permeability contributes to ongoing bowel symptoms in patients with inflammatory bowel disease and mucosal healing. *Gastroenterology* 153, 723–731.e1. <https://doi.org/10.1053/j.gastro.2017.05.056>.
  55. Epple, H.-J., Schneider, T., Troeger, H., Kunkel, D., Allers, K., Moos, V., Amasheh, M., Loddenkemper, C., Fromm, M., Zeitz, M., and Schulzke, J.D. (2009). Impairment of the intestinal barrier is evident in untreated but absent in suppressively treated HIV-infected patients. *Gut* 58, 220–227. <https://doi.org/10.1136/gut.2008.150425>.
  56. Tran, L., and Greenwood-Van Meerveld, B. (2013). Age-associated remodeling of the intestinal epithelial barrier. *J. Gerontol. A Biol. Sci. Med. Sci.* 68, 1045–1056. <https://doi.org/10.1093/gerona/glt106>.
  57. Melamed, E., Rungratanawanich, W., Liangpunsakul, S., Maki, K.A., McCullough, R.L., and Llorente, C. (2025). Alcohol, aging, and the gut microbiome: intersections of immunity, barrier dysfunction, and disease. *Alcohol* 128, 1–12. <https://doi.org/10.1016/j.alcohol.2025.07.001>.
  58. Fábrega, M.J., Aguilera, L., Giménez, R., Varela, E., Alexandra Cañas, M., Antolí, M., Badía, J., and Baldomà, L. (2016). Activation of immune and defense responses in the intestinal mucosa by outer membrane vesicles of commensal and probiotic Escherichia coli strains. *Front. Microbiol.* 7, 705. <https://doi.org/10.3389/fmicb.2016.00705>.
  59. Shi, J., Ma, D., Gao, S., Long, F., Wang, X., Pu, X., Cannon, R.D., and Han, T.L. (2023). Probiotic Escherichia coli Nissle 1917-derived outer membrane vesicles modulate the intestinal microbiome and host gut-liver metabolism in obese and diabetic mice. *Front. Microbiol.* 14, 1219763. <https://doi.org/10.3389/fmicb.2023.1219763>.
  60. Kameli, N., Borman, R., López-Iglesias, C., Savelkoul, P., and Stassen, F.R.M. (2021). Characterization of feces-derived bacterial membrane vesicles and the impact of their origin on the inflammatory response. *Front. Cell. Infect. Microbiol.* 11, 667987. <https://doi.org/10.3389/fcimb.2021.667987>.

61. Tulkens, J., De Wever, O., and Hendrix, A. (2020). Analyzing bacterial extracellular vesicles in human body fluids by orthogonal biophysical separation and biochemical characterization. *Nat. Protoc.* 15, 40–67. <https://doi.org/10.1038/s41596-019-0236-5>.
62. Turrone, F., Duranti, S., Bottacini, F., Guglielmetti, S., Van Sinderen, D., and Ventura, M. (2014). *Bifidobacterium bifidum* as an example of a specialized human gut commensal. *Front. Microbiol.* 5, 437. <https://doi.org/10.3389/fmicb.2014.00437>.
63. Cani, P.D., and de Vos, W.M. (2017). Next-generation beneficial microbes: the case of *Akkermansia muciniphila*. *Front. Microbiol.* 8, 1765. <https://doi.org/10.3389/fmicb.2017.01765>.

STAR★METHODS

KEY RESOURCES TABLE

REAGENT or RESOURCE	SOURCE	IDENTIFIER
<b>Antibodies</b>		
Mouse monoclonal anti-CD63	Thermo Fisher Invitrogen	Cat#10628D; RRID:AB_2532983
Mouse monoclonal anti-CD81	Santa Cruz Biotechnology	Cat#sc-7637; RRID:AB_627190
Rabbit polyclonal anti-OmpA	Abbexa	Cat#abx110631
Donkey-anti-rabbit IRDye®-800CW	LI-COR Biotechnology	Cat#926-32213
Donkey-anti-mouse IRDye®-800CW	LI-COR Biotechnology	Cat#926-32212
<b>Bacterial and virus strains</b>		
Escherichia coli K-12 MG1655	ATCC	47076
<b>Biological samples</b>		
Fecal samples from study participants (adults with prediabetes and overweight, n=12 & healthy adults, n=12)	Maastricht University Medical Center+	NCT03711383
<b>Chemicals, peptides, and recombinant proteins</b>		
Phorbol 12-myristate 13-acetate (PMA)	Sigma-Aldrich	P8139-1MG
β-mercaptoethanol	Merck	1.15433.0050
Phosphate buffered Saline	Gibco	10010023
E.coli O111:B4 LPS	Sigma-Aldrich	LPS25
fetal bovine serum	Bodinco BV	Batch BDC-11933
RPMI 1640 medium	Gibco	11875034
Antibiotic-Antimycotic	Gibco	15240062
Paraformaldehyde	Sigma-Aldrich	8187150100
Glutaraldehyde	Sigma-Aldrich	G5882-50 ML
Methylcellulose/uranyl acetate	Electron Microscopy Sciences	18560
<b>Critical commercial assays</b>		
Human IL-1 beta Uncoated ELISA Kit	Invitrogen	88-7261-88
Human TNF alpha Uncoated ELISA Kit	Invitrogen	88-7346-88
Human IL-6 Uncoated ELISA Kit	Invitrogen	88-7066-88
QIAmp DNA Mini Kit	Qiagen	51306
PicoGreen Quant-iT	Invitrogen	P7589
AMPure XP beads	Beckman Coulter	A63881
MiSeq V3 reagent kit	Illumina	MS-102-3003
Qubit dsDNA quantification assay kit	Invitrogen	Q32852
AccuPrime High fidelity DNA polymerase	Thermo Fisher Scientific	12346086
<b>Deposited data</b>		
16S rRNA gene amplicon sequencing data	European Nucleotide Archive (ENA)	Accession: PRJEB96207
<b>Experimental models: Cell lines</b>		
THP-1 monocytes	ATCC	TIB-202, RRID: CVCL_0006
<b>Oligonucleotides</b>		
16S rRNA gene V4 primer 515 Forward	Eurofins	5'-GTGCCAGCMGCCGCGGTAA-3'
16S rRNA gene V4 primer 806 Reverse	Eurofins	5'-GGACTACHVGGGTWTCTAAT-3'
<b>Software and algorithms</b>		
R	R foundation	V4.2.0
DADA2	Bioconductor	V1.28.0

(Continued on next page)

**Continued**

REAGENT or RESOURCE	SOURCE	IDENTIFIER
microViz	<a href="https://github.com/avid-barnett/microViz">https://github.com/avid-barnett/microViz</a>	V0.12.1
GraphPad Prism	GraphPad	V8.02
IMAGEsTUDIO	LI-COR Biotechnology	V6.1
<b>Other</b>		
ZetaView NTA	Particle Metrix	PMX 120
qEV 35 nm SEC columns	IZON	qEV35
Tecnai Arctica Cryo-TEM	Thermo Fisher Scientific	-
Tecnai G2 Spirit TEM	Thermo Fisher Scientific	-
Illumina Miseq Sequencer	Illumina	MiSeq
Spectramax platereader	Molecular Devices	iD3
Optima L-100K Ultracentrifuge	Beckman Coulter	Optima L-100K
Quick-Seal Centrifuge tubes	Beckman Coulter	342412
Millex syringe filter 0.22 $\mu$ m	Millipore	SLMP025SS
Amicon Ultra centrifugal filter unit, 100 kDa MWCO	Millipore	UFC910024
Polystyrene beads 100 nm	Particle Metrix	Art. 110-0020
Formvar/carbon-coated copper grids	Electron Microscopy Sciences	FCF200-Cu
Vitrobot Mark IV	Thermo Fisher Scientific	-
Zephyr NGS Automated Workstation	PerkinElmer	Zephyr G3
Qubit fluorometer	Thermo Fisher Scientific	Qubit 3.0
6 well polystyrene culture plates	Greiner	657160

**EXPERIMENTAL MODEL AND STUDY PARTICIPANT DETAILS**

**Human subjects**

Fecal samples were collected from Caucasian male participants diagnosed with prediabetes ( $n = 12$ ) and healthy normoglycemic controls ( $n = 12$ ). Prediabetic participants were included based on a BMI  $> 25 \text{ kg/m}^2$  and impaired fasting glucose (plasma glucose  $\geq 6.1 \text{ mmol/L}$  and  $\leq 7.0 \text{ mmol/L}$ ) and/or impaired glucose tolerance (plasma glucose  $\geq 7.8 \text{ mmol/L}$  and  $\leq 11.0 \text{ mmol/L}$ ). Healthy controls were included based on a BMI between 20 and  $24.9 \text{ kg/m}^2$ , fasting plasma glucose  $< 6.1 \text{ mmol/L}$ , and normal glucose tolerance (plasma glucose 2 h post ingestion of a 75 g glucose beverage  $< 7.8 \text{ mmol/L}$ ).

Fecal samples were self-collected at home and immediately frozen. Sample collection was approved by the Medical Ethical Committee of Maastricht University Medical Center and monitored by the Clinical Trial Center Maastricht (NCT03711383). All participants provided written informed consent.

**Cell-lines**

THP-1 monocytes (ATCC TIB-202, from a male patient) were used for *in vitro* stimulation experiments.

**METHOD DETAILS**

**Fecal bacterial DNA extraction**

Stored fecal samples (0.5 g) were thawed and resuspended in 5 mL sterile PBS and centrifuged at  $5,000 \times g$  for 15 min at  $4^\circ\text{C}$  to pellet bacteria. Pellets were subjected to bead-beating and column-based DNA extraction using the QIAmp DNA Mini Kit (Qiagen, 51306).

**Bacterial membrane vesicle isolation and purification**

Bacterial membrane vesicles (bMVs) were isolated using consecutive ultracentrifugation and size exclusion chromatography steps. Fecal samples (0.5 g) were suspended in PBS and centrifuged at  $5,000 \times g$  for 15 min at  $4^\circ\text{C}$ . Supernatants devoid of bacteria were ultracentrifuged at 40,000 rpm for 150 min at  $4^\circ\text{C}$  under vacuum to pellet bMVs. Pellets were resuspended in PBS, filtered through 0.22  $\mu\text{m}$  filters, and concentrated by ultrafiltration (100 kDa MWCO at 4000G (room temperature, 1 minute intervals). 500  $\mu\text{L}$  concentrates were subjected to SEC using qEV 35 nm columns, and 1 mL fractions 4–6 were pooled and stored at  $-80^\circ\text{C}$ .

**Nanoparticle tracking analysis**

Particle size and concentration were determined using a ZetaView PMX 120 nanoparticle tracking analyzer (Particle Metrix). Calibration was performed using 100 nm polystyrene beads (Particle Metrix, Art. 110-0020). Samples were diluted 1:500 in PBS (Gibco, Cat#

10010023) prior to measurement. Measurements were performed at room temperature and analyzed using ZetaView software (Particle Metrix).

### Western blot analysis

Vesicle protein was analyzed by western blotting for CD63 (1:1,000, non-reducing conditions), CD81 (1:1,000, non-reducing conditions), and outer membrane protein A (OmpA; 1:2,500, reducing conditions) (Table S2 and Figure S5). Samples were prepared in 6× Laemmli sample buffer (G-Biosciences, Cat# 786-701) with or without β-mercaptoethanol (Merck, Cat# 1.15433.0050) depending on reducing conditions. Equal particle numbers ( $5 \times 10^8$  vesicles) were loaded onto 4–12% Criterion XT Bis-Tris gels (Bio-Rad, Cat# 345-0124) using XT MES running buffer (Bio-Rad, Cat# 161-0789). Precision Plus Protein Standards All Blue (Bio-Rad, Cat# 161-0373) were used as molecular weight markers. Proteins were transferred to 0.45 μm nitrocellulose membranes (GE Healthcare, Cat# RPN303D) at 100 V for 1 h. Membranes were blocked for 1 h in Intercept blocking buffer (LI-COR, Cat# 927-70001). Proteins were detected using fluorescently labeled secondary antibodies (1:10,000) and imaged on an Odyssey Infrared Imaging System (LI-COR). All antibodies were diluted in TBS containing 0.1% Tween-20. Image acquisition and analysis were performed using Image Studio software (LI-COR).

### Negative-staining transmission electron microscopy

Purified bMVs were deposited on Formvar/carbon-coated copper grids (Electron Microscopy Sciences) at approximately  $1 \times 10^{10}$  vesicles/mL and incubated at room temperature for 20 min. Grids were fixed with 2% paraformaldehyde and 1% glutaraldehyde in 100 mM phosphate buffer for 20 min, washed with water, and contrasted with methylcellulose/uranyl acetate (Electron Microscopy Sciences) for 10–12 min on ice. Excess liquid was removed by blotting and grids were air-dried. Grids were examined using a Tecnai G2 Spirit transmission electron microscope (Thermo Fisher Scientific) operated at 120 kV.

### Cryo-transmission electron microscopy

Three microliters of purified bMV suspension were applied to glow-discharged holey carbon grids (Electron Microscopy Sciences). Grids were maintained at 95% humidity, blotted with filter paper, and plunge-frozen in liquid ethane using a Vitrobot (Thermo Fisher Scientific). Vitrified samples were transferred to a Tecnai Arctica cryo-transmission electron microscope (Thermo Fisher Scientific) operated at 200 kV.

### 16S rRNA gene amplification and sequencing

For bacterial and vesicle-associated DNA, amplification of the 16S rRNA gene variable region followed by Illumina sequencing was performed. The V4 region was amplified using primers 515F (5'-GTGCCAGCMGCCGCGGTAA-3') and 806R (5'-GGACTACHVGGGTWTCTAAT-3'), synthesized by Eurofins, Netherlands. PCR mixes (50 μL total reaction volume) contained 1 μL of each primer (10 pmol/μL), 0.2 μL AccuPrime High Fidelity DNA polymerase (Thermo Fisher Scientific), 5 μL AccuPrime buffer II, 1 μL template DNA, and 41.8 μL water. PCR cycling conditions consisted of an initial denaturation at 94°C for 3 min, followed by 35 amplification cycles for bMV DNA templates or 25 cycles for bacterial DNA templates (94°C for 30 s, 50°C for 45 s, and 72°C for 60 s), and a final extension at 72°C for 10 min. Amplicon size and quality were verified on 1% agarose gels. Amplicon libraries were purified using Agencourt AMPure beads on a Zephyr G3 NGS automated workstation (PerkinElmer). DNA concentrations were quantified using PicoGreen Quant-iT (Invitrogen), and libraries were pooled at equimolar concentrations to a final concentration of 1 ng/μL. Sequencing was performed on an Illumina MiSeq system using the MiSeq v3 reagent kit.

### Cell culture stimulation and harvest

THP-1 monocytes (ATCC TIB-202, RRID: CVCL\_0006) were seeded in 6-well polystyrene culture plates (Greiner) at a density of  $3 \times 10^5$  cells/mL in 2 mL RPMI 1640 medium (Gibco, Cat# 11875034) supplemented with 10% fetal bovine serum (Bodinco BV, Batch BDC-11933) and 1× Antibiotic-Antimycotic (Gibco, Cat# 15240062). Cells were differentiated with phorbol 12-myristate 13-acetate (PMA; Sigma-Aldrich, Cat# P8139-1MG) at 50 ng/mL for 24 h at 37°C in 5% CO<sub>2</sub>. Cells were washed and incubated for an additional 24 h in unsupplemented RPMI 1640 medium prior to stimulation.

Cells were stimulated with purified bMVs at  $5 \times 10^7$  vesicles per well for 24 h at 37°C in 5% CO<sub>2</sub>. Conditioned media were collected for cytokine quantification by ELISA.

### Cytokine ELISA

Conditioned media were analyzed using human uncoated enzyme-linked immunosorbent assay (ELISA) kits for IL-6, TNFα, and IL-1β (Thermo Fisher Scientific; catalog numbers listed in the [key resources table](#)). For each assay, wells were pre-coated with 100 μL of capture antibody and incubated at 4°C overnight. The next morning, wells were washed, and 100 μL of sample or standard was added and incubated at room temperature for 2 h. After washing, 100 μL of detection antibody was added and incubated for 1 h. After washing, 100 μL of HRP-conjugated (strept)avidin was added and incubated for 30 min. Plates were washed and developed with 100 μL of TMB substrate. Reactions were terminated by addition of 100 μL stop solution after 15 min, and absorbance was measured at 450 nm using a Spectramax iD3 platereader (Molecular Devices). Cytokine concentrations were calculated from standard curves.

## QUANTIFICATION AND STATISTICAL ANALYSIS

### Sequencing data processing

Amplicon data were processed using DADA2 (v1.28.0) and classified using the SILVA 138.1 database. Downstream analysis was performed in R (v4.2.0) using microViz (v0.12.1).

### Statistical analysis

Group-based differences in beta-diversity were assessed using PERMANOVA with Bray–Curtis distances at the genus level. Bacterial richness, diversity, and relative abundances were compared using Mann–Whitney tests. Cytokine data and group parameter comparisons were analyzed using unpaired two-tailed t tests. Statistical analyses were performed in RStudio (v2024.04.0+735) and GraphPad Prism (v8.02), with  $\alpha = 0.05$ .